Experimental analysis of CO_2 frost front behaviour in moving packed beds for cryogenic CO_2 capture

David Cann[a], Carolina Font-Palma[a,*], Paul Willson[b]

[a] Department of Chemical Engineering, University of Chester, Chester, CH2 4NU, UK

[b] PMW Technology Limited, Thornton Science Park, Ince, Chester, CH2 4NU, UK

Abstract

In this work, the feasibility of a novel method of cryogenic carbon capture based on carbon dioxide frost deposition onto a cold moving bed is explored. As a gas mixture including CO_2 flows through a sufficiently cold packed bed, CO_2 is deposited onto the bed material as a frost. As the bed is warmed by the gas stream the frost front advances through the bed. Experimental measurements of the rate of frost advance within a static packed bed are used to set up a moving bed to achieve continuous CO_2 removal. Precooled and dry binary gas mixtures of CO_2 and nitrogen are used to determine frost front velocity in a capture column. The frost front velocity measured in fixed bed experiments with varying CO_2 concentrations and gas flow rates are in the range of 0.4 to 1 mm/s. The experimental results were used to design a moving bed system that would match this range of frost front velocities so that continuous capture would be possible. Experiments were conducted to investigate the behaviour of temperature profiles within the capture column under moving bed conditions. These show that frost accumulation does not occur and successfully demonstrates continuous cryogenic carbon capture.

Keywords: carbon capture, cryogenic separation, moving bed, desublimation

1. Introduction

* Corresponding author: C.Font-Palma@hull.ac.uk. Present address: Department of Engineering, University of Hull, Hull, HU6 7RX, UK

Increased concerns over climate change has led governments to invest in climate change mitigation technologies. CO_2 abatement such as carbon capture and storage (CCS) and carbon dioxide removal (CDR) are agreed to be necessary in order to meet climate targets of 2^oC and below at the lowest cost [1, 2]. CCS was firstly proposed for the energy sector as a method to decarbonise fossil fuels [3], but now the focus is attracting attention as a method to decarbonise other industries such as cement making and biogas purification [4, 5].

In the UK, the government aims to capture 10Mt of CO_2 per year by 2030 through carbon capture and utilisation and storage (CCUS) technology, with a further pledge to reduce greenhouse gas emissions by 100% relative to 1990 levels by 2050 as an amendment to the 2008 climate change act, which had previously made a commitment to reduce emissions by 80% [6]. The UK will focus on hotspots of industrial activity for CCUS development, known as industrial clusters, such as the Net Zero Teeside and Zero Carbon Humber projects. These industrial clusters will reduce the cost of CCUS by providing economies of scale [2]. The EU also plans to implement commercial scale CCS within the energy and industrial sectors in the 2020s, acknowledging the role of CCS in the IPCC 1.5^oC special report [7].

1.1. Cryogenic carbon capture

Post-combustion carbon capture technology has an important advantage of being able to be retrofitted onto existing power plants and industries [3]. Of these post-combustion technologies, chemical absorption is the most established and mature technology [1]. A significant disadvantage of absorption using amine-based solutions is that the process requires large equipment sizes with difficulties in scaling down economically for industrial applications [8]. For these industries, other methods of post-combustion carbon capture need to be explored [4]. The requirement for low carbon technologies across various industries increases as the energy sector continues to decarbonise.

Cryogenic carbon capture (CCC) is a technology that can operate at smaller scale and has been considered both in carbon capture for cleaning flue gases [9, 10] and biogas upgrading [11]. CCC operates through a physical phase change of CO_2, meaning that no absorbent is required.

Furthermore, the application of cryogenic packed beds allows for CO_2 capture at low pressure. These key advantages have driven research into CCC [5, 9, 12-14]. CCC often features a fixed heat transfer surface to cool down the CO_2 sufficiently to cause desublimation and frost deposition [9, 14]. Once the heat transfer surface is saturated with frost, heat must be applied to regenerate the heat transfer surface and recover CO_2. This regeneration step requires periodic shut down of the capture step; the overall process would require multiple capture columns operating cyclically to capture CO_2 continuously [15], increasing capital cost substantially.

1.2. Moving bed for cryogenic carbon capture

A significant limitation of CCC is the loss of heat transfer efficiency as CO_2 frost develops on the heat transfer surface [15, 16]. As a solution to overcome this limitation, a novel advanced cryogenic carbon capture process that uses a moving packed bed to perform heat transfer has been proposed. This moving bed process, known as Advanced Cryogenic Carbon Capture (A3C), comprises three major unit operations; a chilling step to cool the gas and reduce the water vapour content, a recuperative cooler-drier stage which cools the gas and removes the remaining water vapour, and a CO_2 separation stage which separates CO_2 from the flue gas and captures it as a frost on a moving bed [11]. The refrigeration required for bed cooling would be conventional but would be closely integrated with the process heat demand for CO_2 sublimation at around 196K, reducing the overall energy consumption significantly.

The technical and economic feasibility of the A3C process has been assessed through modelling and economic analyses [11], in which it was compared on a consistent basis with amine-based CO_2 capture for a number of potential applications. A common observation for existing CCC is that it has a high energy consumption for the necessary refrigeration. The appeal for the highly recuperative A3C process is that it minimises this energy demand, with the feasibility study showing a specific energy consumption for CO_2 capture of 263 kWh/ tonne for biogas upgrading applications [11]. An outline of the A3C separation is provided in figure 1.

The feasibility study highlights biogas upgrading as a potential application that is favourable to the A3C process in comparison to small scale amine-based absorption. This solidified the process at a technological readiness level (TRL) of 2-3 [1]. This work is focused on the control of frosting in the desublimer unit of the CO_2 separation stage. The desublimer is the critical unit operation of the A3C process, demonstration of the moving bed process with experimental tests would validate the A3C process at TRL 3. Allowing advancement from the research focused TRLs to development focused TRLs [1].

The movement of the bed in the separation step allows CO_2 to be recovered from the frosted bed material by warming outside of the capture column and then cooled it again for return to the capture column. This moving bed system would prevent the build-up of CO_2 frost within the capture column, eliminating the need for multiple capture columns for continuous operation and improving the heat transfer efficiency of the process.

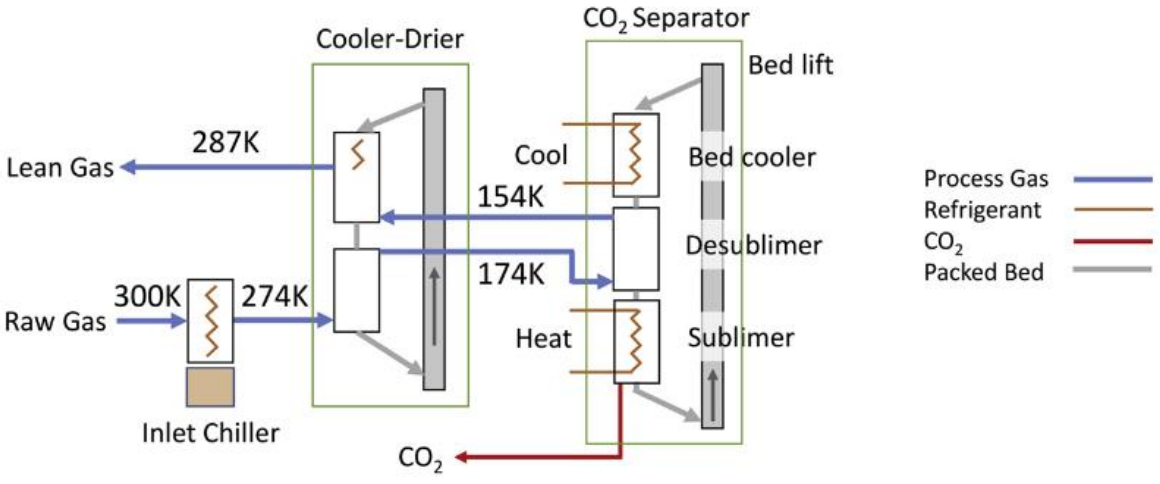

Figure 1. Outline of the two stages of A3C separation process, temperatures refer to a flue gas application [11] (colour)

This work aims to expand upon previous CCC studies and connect it to the moving bed processes [17-19] as to date there are no studies combining these two aspects. Another research gap is a lack of

studies on fundamentals of CO_2 frost formation within a packed bed and how it interacts with heat transfer. Measuring heat transfer in a moving bed while measuring and factoring CO_2 frost development presents a set of unique challenges, which will have to be addressed.

The first challenge is the frost front velocity, the velocity at which the frosted region in a static packed bed advances up the column. The moving bed would have to match this frost front velocity to form an equilibrium frost front. Therefore, this work presents experiments conducted to investigate the frost front velocity within a purposely built experimental rig which allows experiments with either static or moving packed beds. In static operation, the experimental set up is similar in design to work done by Tuinier et al. [9]. Tuinier et al. injected a mixed gas of nitrogen, CO_2 and water vapour into a pre-cooled capture column with the difference in dew and sublimation points of CO_2 and water causing the two components to form separate frost fronts which advanced through the column at different velocities. The fixed packed bed experimental results from this work are used to construct frost front velocity curves which are then compared with results from Tuinier et al [9, 15] for validation. Then, moving bed experiments are presented for the first time to investigate whether the frost front velocity can be controlled.

2. Materials and Methods

The cryogenic cooling column was designed as a 1m tall vertical column made of PTFE, ID=0.072m, OD=0.095m. The column is held between two aluminium plates with orifices to allow the filling and emptying of bed material in the column. A sketch of the rig is presented in figure 2.

The bed material consists of small, approximately spherical, stainless steel beads used commercially for shot peening. These were sifted to ensure that the material consists of particles with a diameter of 1.4-1.7mm. Furthermore, the bed porosity within the column was calculated as 0.42 by weighing test samples of bed material occupying a known volume.

Two GSS ExplorIR®-W CO_2 sensors record CO_2 concentrations with a precision of 0.001% and type-K thermocouples attached to dataloggers (TC-Direct 4 channel) record temperature inside the column at different heights above the gas injector. The gas injector is a perforated copper pipe that rests inside the cooling column, distributing the gas stream across the column. The copper pipe is perforated with 1mm wide radial slits on opposite sides of the pipe.

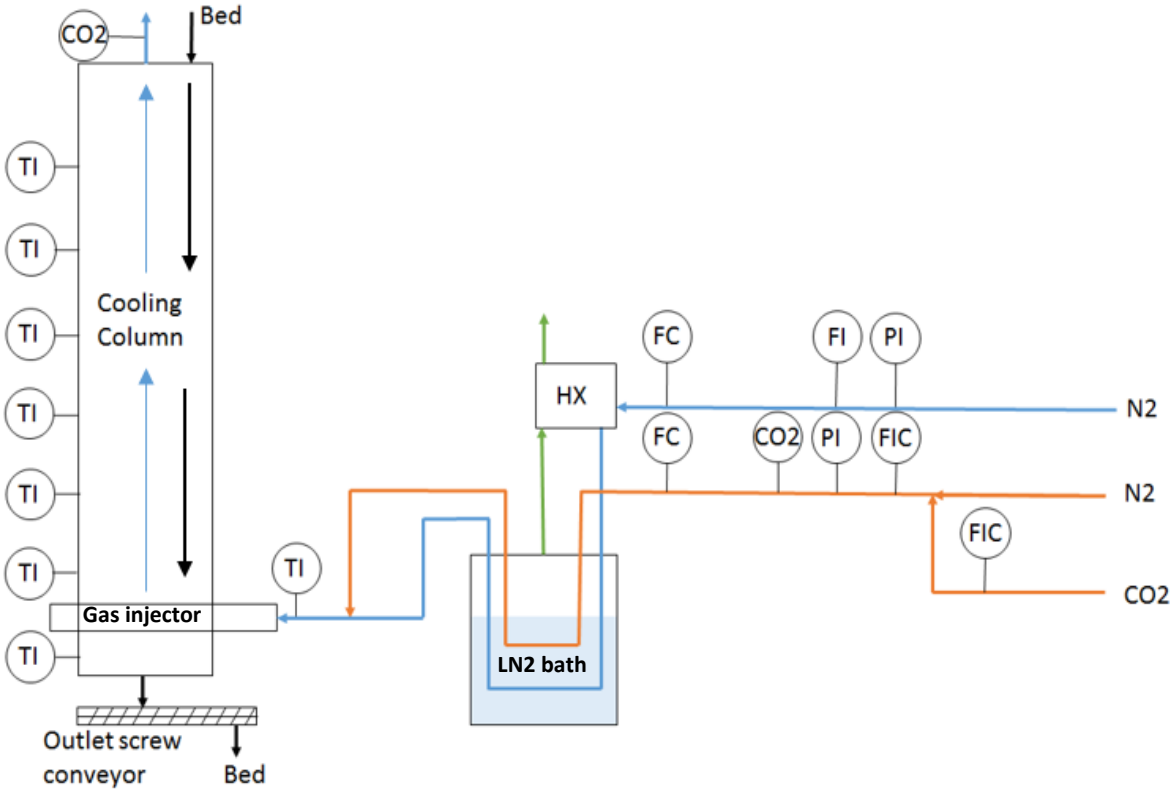

Figure 2. Sketch of moving bed experimental set up. (colour)

Figure 2 shows a liquid nitrogen (LN2) bath used to cool down the gas streams, with the heat exchanger (HX) utilising the low temperature nitrogen vapour for further cooling. Liquid nitrogen was used as the refrigerant for the cooling gas due to its ease of use for experiments at this scale where energy consumption was not a focus of this work. The nitrogen and CO_2 gases are supplied from high pressure cylinders, with purities of over 99.98% and 99.8% respectively. The nitrogen stream (blue) is cooled to roughly -140^{o}C and is used to cool down the bed material until it reaches -120^{o}C. The cooled

nitrogen gas is injected directly into the capture column filled with metal bed material. The gas stream is then switched to the mixed gas line (orange) of CO_2 and nitrogen, which is cooled to roughly -75^{o}C. The gas is first pre-cooled to close to the saturation temperature for CO_2 deposition so that the more intensive cooling by the moving bed in the separation step can be matched to the energy required for desublimation. The gas mixture is then cooled further by the moving bed to desublimate CO_2, causing frost to form on the bed material. The mixed gas line is controlled using manual flow control valves to regulate the flow rates of the CO_2 and nitrogen gas lines which are then mixed. The total flow rate and CO_2 composition of the mixed gas is measured using a rotameter and a GSS sensor.

The frost front velocity for fixed bed experiments was measured under a range of different gas flow rates and CO_2 concentrations, as shown in table 1.

Table 1. Frost front velocity experimental conditions

Inlet gas flow rate (LPM)	Superficial velocity (m/s)	Inlet gas CO_2 concentration (% v/v)
100	0.23	18
100	0.23	8
100	0.23	4
120	0.28	18
80	0.18	18
50	0.12	18

The superficial velocities are dependent on the temperature of the gas, with colder gas temperatures resulting in a higher density of gas and thus reducing the superficial velocity within the column. The superficial velocity was calculated using a temperature approximate to the desublimation

142 temperature of CO_2 within the gas phase in order to calculate the superficial velocity of the mixed gas
143 in the column prior to desublimation.

144 For moving bed experiments, a purpose built screw conveyor was placed at the bottom of the capture
145 column with a variable speed motor. The speed of the motor can be adjusted to alter the RPM of the
146 screw conveyor and therefore control the flow rate of the bed material. The outlet for the bed was
147 designed to ensure that the bed material has a consistent rate of movement at all distances from the
148 centre with minimal mixing of the material.

149 The moving bed experiments were conducted using a gas superficial velocity of 0.17 m/s and a CO_2
150 concentration of 18%. This gas flow rate was set to match the bed flow rate measured for the screw
151 conveyor at 200 RPM at ambient conditions, providing a bed mass flow rate of 0.024 kg/s and vertical
152 velocity of about 1 mm/s. Moving bed experiments recorded the temperature profiles of the 5mm
153 and 30mm thermocouples with bed inlet temperature of -140^{o}C. The conditions for the moving bed
154 experiments are summarised in table 2. The outlet gas sensor set up was modified to collect and
155 measure gas samples close to the frost front. A small pipe was inserted to the 30mm point connected
156 to the gas sensor at the capture column outlet, which would allow gas samples close to the frost front
157 to be measured by the GSS sensor. The 30mm thermocouple was placed inside the gas sampling pipe
158 to measure the temperature at the same point.

159 **Table 2.** Moving bed experimental conditions

Initial bed temperature (^{o}C)	-140
Bed flow rate (RPM)	200
Bed mass flow rate (kg/s)	0.024
Bed vertical velocity (mm/s)	1
Superficial velocity gas (m/s)	0.17
Gas CO_2 concentration (% v/v)	18

160

After the initial cooling step was completed in each experiment, bringing the bed to the desired temperature, the flow of cooling N_2 gas was stopped and the screw conveyor started to remove bed material from the capture column at a fixed rate. Shortly after, the mixed gas was fed by the gas injector. Thermocouples at 5mm and 30mm points were used to measure the temperature of the bed material close to the injector, where it is believed that the frost front will remain static in place as opposed to advancing further up the column.

3. Results and discussion

3.1 Fixed bed temperature profiles

Figure 3 shows a selection of results from the cryogenic packed bed experiments used to determine frost front velocity. Figure 3ai and 3bi show the temperatures of the bed material at certain distances above the gas injector where the flue gas is introduced to the cooling column. The plateaus that form after initial temperature change indicate frost deposition onto the bed material. The time at which the plateaus form at each of the thermocouples are used as reference points for measuring frost front velocity.

ai)

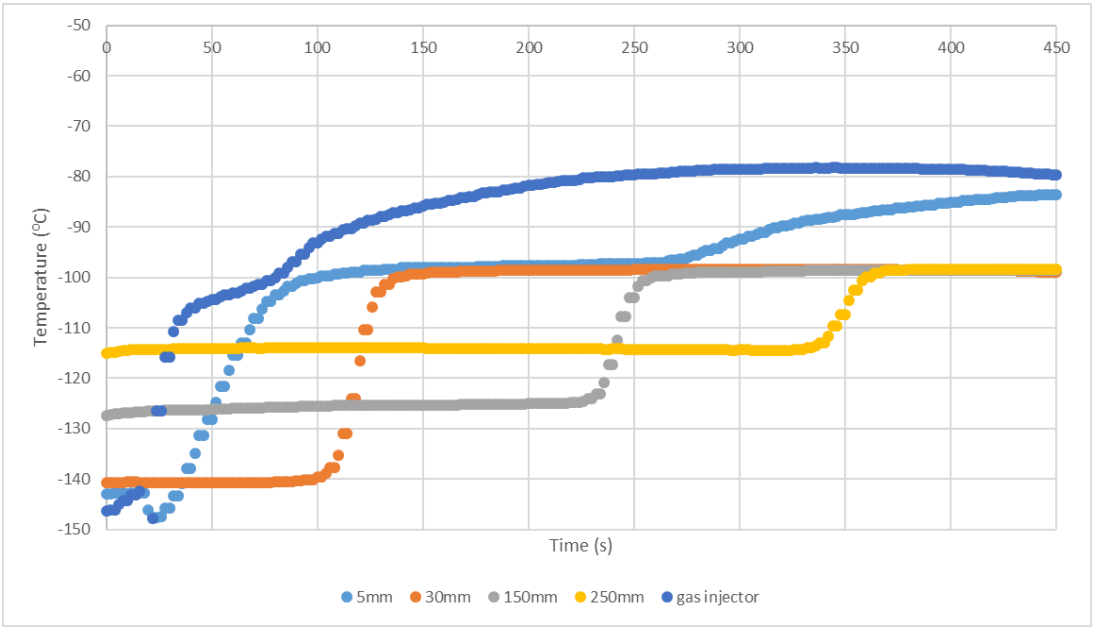

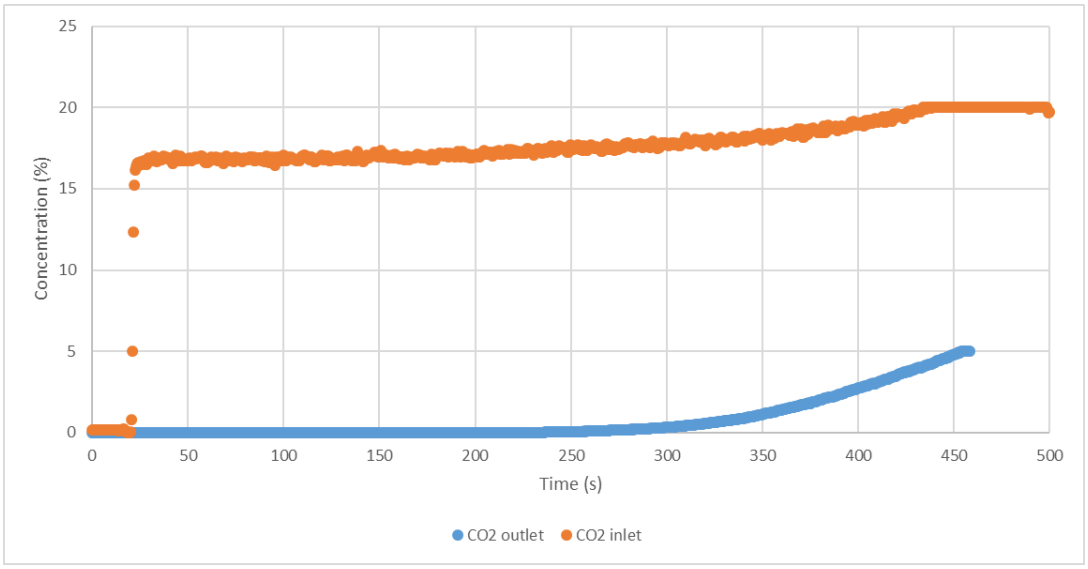

176 aii)

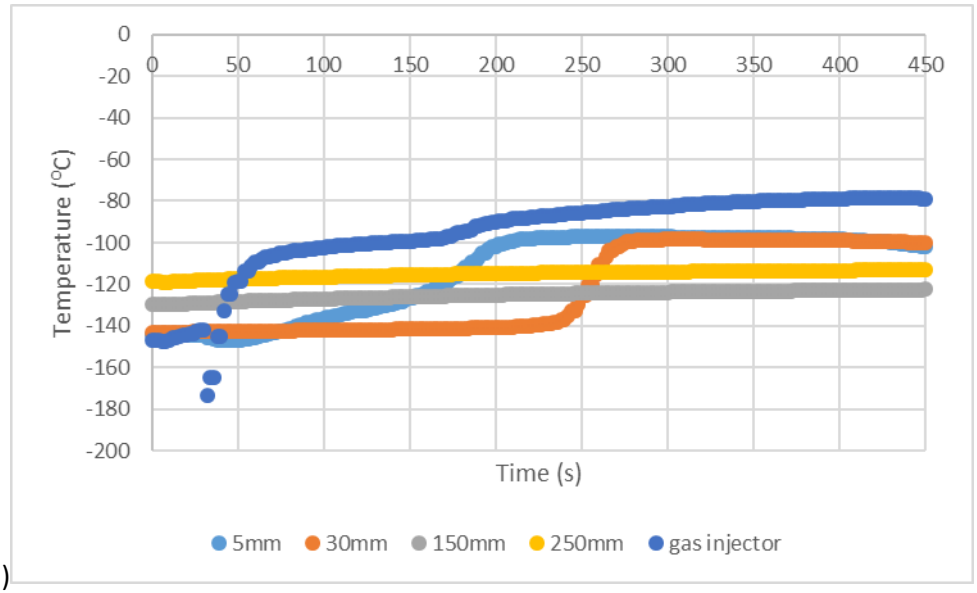

177 bi)

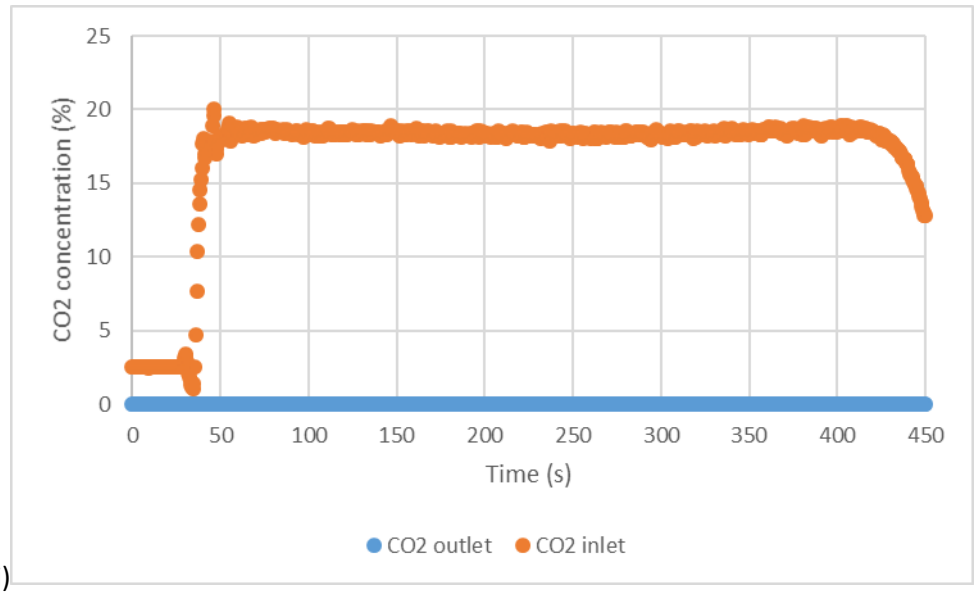

178 bii)

Figure 3. Temperature readings from gas injector and different heights in the column and CO_2 sensor measurements from a) 100LPM, 0.23 m/s, 18%, b) 50LPM, 0.12m/s, 18% (colour)

The results in figure 3 show CO_2 removal within the column during each experiment ranging from 93% to 100% (or CO_2 levels below the detection limit). Figure 3aii and 3bii show the concentration of CO_2 in the mixed gas before entering the packed bed and after exiting the packed bed. Almost all CO_2 is captured until the final moments of each experimental run, which is the point where the packed bed material entirely reaches the plateaued temperature. It can be seen that the point in time when the CO_2 concentration exiting the column starts to rise occurs roughly at the same time that the frost front has advanced 250mm up the column.

The time at which the plateaus form for each temperature profile gives an indication of how fast the frost front is advancing through the capture column. From figure 3ai and 3bi, the 0.23 m/s superficial velocity results in a faster frost front velocity as the temperature profiles plateau earlier than can be seen in the 0.12 m/s temperature profiles. At the lower flow rate temperature profiles for the 150mm and 250mm thermocouples do not plateau after 450s, indicating that the frost front never advanced that far up the column during the experiment.

Figure 4 shows the averaged results of the frost front experiments and presents the frost front velocity under different gas flow rates and CO_2 concentrations. The gradients of each line represent the frost front velocity inside the cooling column at a rate of mm/s.

a)

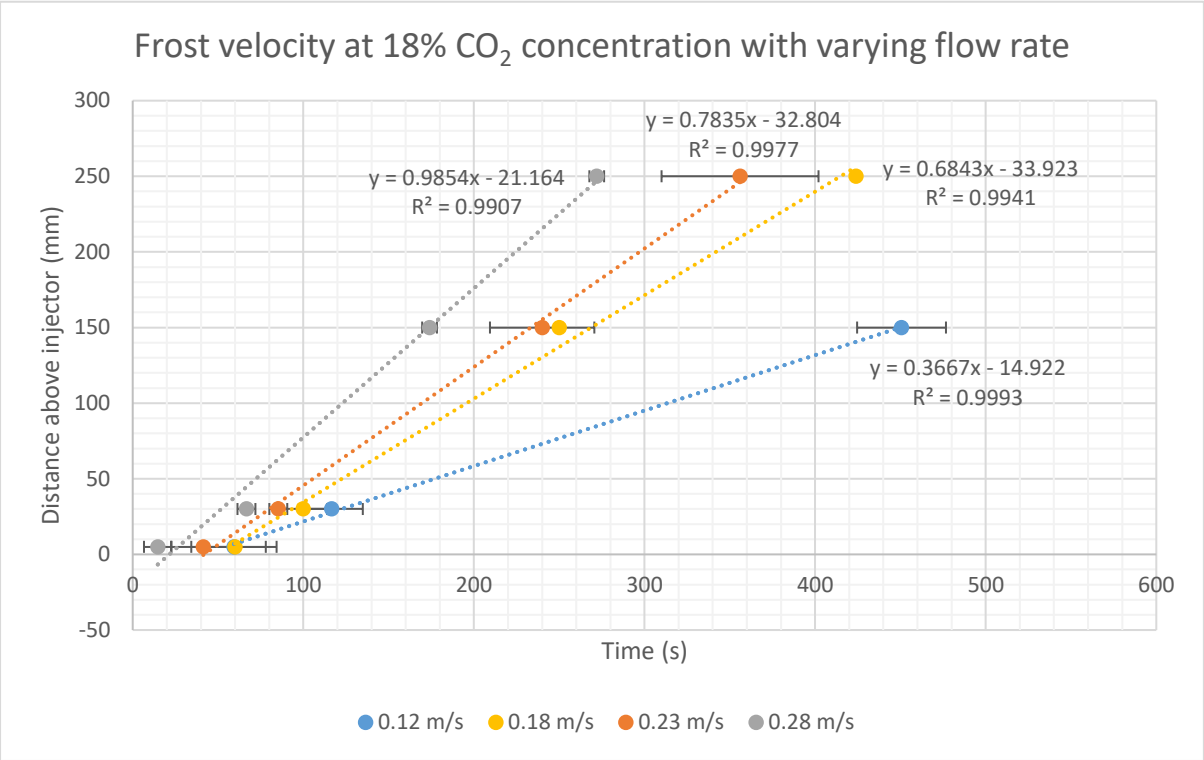

b)

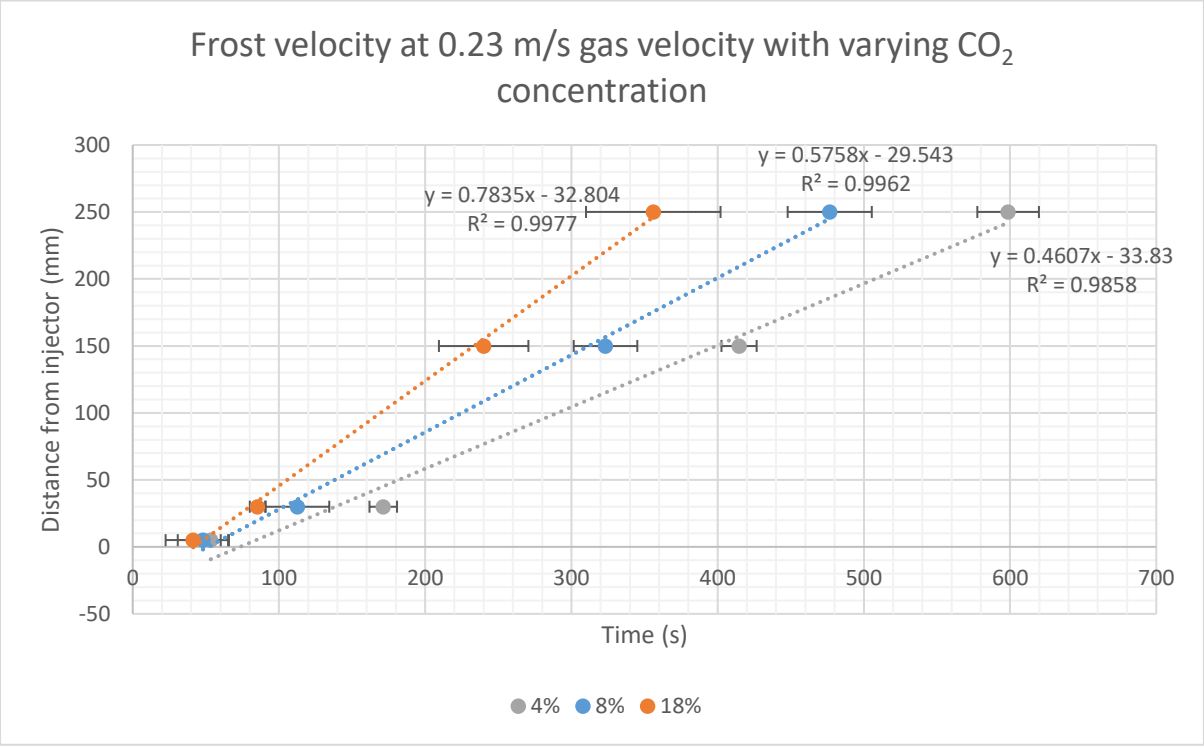

Figure 4. Frost front velocities under different conditions a) frost front velocities for different gas superficial velocities, b) frost front velocities for different CO_2 concentrations. (colour)

The range of frost front velocity varies between 0.46-0.78 mm/s with varying CO_2 concentrations ranging from 4%-18% and between 0.37-0.99 mm/s with varying gas superficial velocities ranging from 0.12-0.27 m/s. The trendlines shown in figure 4 do not intercept the y-axis at zero, this is likely indicative of supercooling effects where the incoming flue gas is cooled but there is no point of nucleation for CO_2 frost deposition to occur. It should be noted however, that the magnitude of the difference in where the y-axis is intercepted is dependent on the assumption of t_0 and the beginning of the experiment. For the purpose of these experiments, t_0 is assumed to be the time at which the temperature of the flue gas entering the column, shown by the gas injector thermocouple, reached the temperature that CO_2 would desublimate for the given gas composition.

3.2 Comparison with literature and modelling

The experimental work was compared with a theoretical model based on the conservation of energy over the frost region. This model was used to predict the frost front velocity within the capture column under different gas flow rates and CO_2 compositions. The theoretical model is summarised by equation (1) given below.

$$U_{frost} = \frac{Q_g}{A\rho_s c_{ps} \Delta T} \quad (1)$$

where U_{frost}=frost front velocity, Q_g is the cooling duty required for the CO_2 present in the gas to desublimate, A is the cross sectional area of the column, ρ_s is the density of the bed material, $c_{p,s}$ is the specific heat capacity of the bed material and ΔT is the temperature change of the bed material from initial bed temperature to frosted bed temperature.

The fixed bed experimental results from experiment were also compared with results from Tuinier et al [9, 15], CO_2 temperature profiles from their experimental work were used to estimate frost front velocities. The capture columns used in the different sets of experiments differ, thus correction factors were used in order to better compare the two sets of results using equation (2).

235 The overall correction factor was predicted to be as follows:

236 $$\frac{dvdy}{d\rho dc_p} \quad (2)$$

237 where *y* is the volume fraction of CO_2 in the gas phase and *v* is the gas superficial velocity. The relative
238 differences between the sets of experimental data are compiled in table 3.

239 **Table 3.** Correction factors for experimental results

Characteristic	Tuinier [9]	This work	Correction factor
Superficial gas velocity (m/s)	0.1	0.23	2.36
CO_2 composition (% v/v)	20	18	0.9
Bed material	Glass	Steel	
Density of bed material (kg/m^3)	2547	7850	3.08
Specific heat capacity during capture step (J/kgK)	365.4	400	1.10

240

241 The results in Tuinier et al.'s work allow an estimate for the frost front for a small range of results, the
242 frost front velocity for 20% CO_2 at 10LPM was estimated to be 1.37mm/s. The correction factors allow
243 the frost front velocity to be converted to an approximate frost front velocity for different gas flow
244 rates. Differences in concentration were kept minimal by comparing 10% and 20% CO_2 results from
245 Tuinier et al. and 8% and 18% results from this work respectively. Comparisons are shown in figure 5.

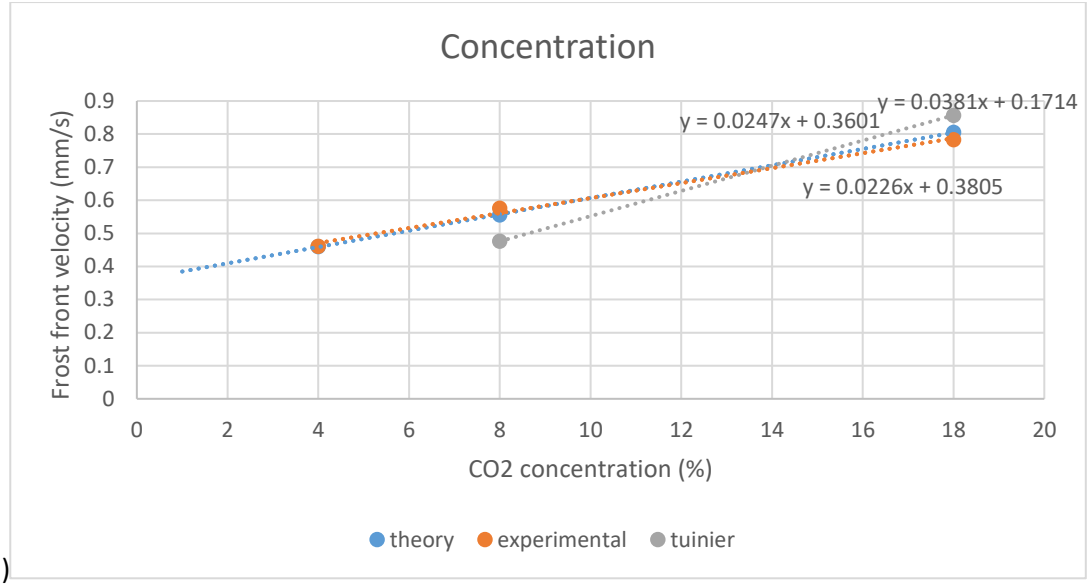

a)

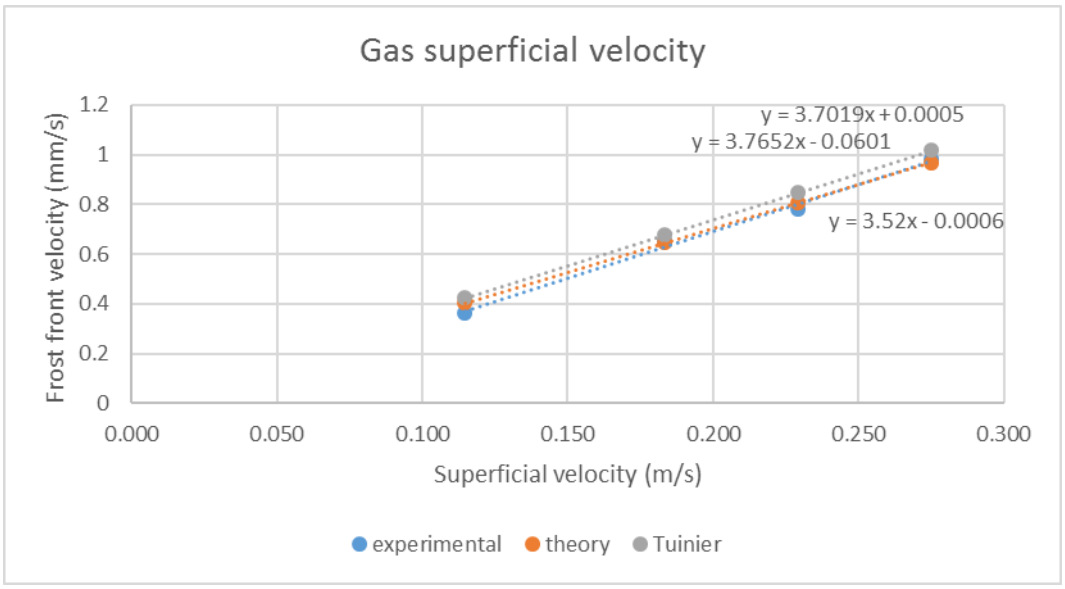

b)

Figure 5. Comparison between theoretical modelling predictions, experimental work and results estimated from Tunier et al. [9, 15] a) frost front velocity trend based on CO_2 concentration in mixed gas b) frost front velocity trend based on gas superficial velocity. (colour)

In figure 5a, the gradient 0.0226 is for experimental results, 0.0247 is for theoretical modelling and 0.0381 is for Tuinier et al. corrected values; in figure 5b the gradient 3.52 is for the theoretical modelling, 3.7019 is for experimental work and 3.7652 is for Tunier et al corrected values. The trends in figure 5 show a good level of agreement between the sets of results, especially between the

theoretical modelling predictions and the experimental results; however, there is less reliability in comparisons between experimental and literature data with changing concentration. Thus, it is possible to make a relatively simple comparison between different sets of experimental results as long as the concentration of CO_2 in the flue gas and initial bed temperatures are similar. This method of using correction factors to accommodate for discrepancies in CO_2 concentration is only suitable for relatively small changes in concentration, as altering the CO_2 concentration in the flue gas will alter the desublimation temperature of the CO_2, which then affects the temperature change of the bed material and gas phase through the capture column.

3.3. Moving bed experiments

The fixed bed experimental measurements shown in Figure 5 were used to predict the frost front velocity so that the bed flow could be set to stop front movement at the gas conditions for the moving bed experiments.

The moving bed aims to balance the accumulation of frost within the bed material by removing frosted bed from the capture column. The relationship between the bed and frost front velocities allow a comparison between the mass flow rates of CO_2 and the bed material. Assuming that all the CO_2 is deposited as frost under conditions given in table 2 indicates that the CO_2 frost mass flow rate is 1.78% that of the bed material flow rate. This is in agreement with earlier work done on the A3C process [11]. In other words, mass of CO_2 frost desublimed on the bed material is 1.78% of the mass of the bed material itself. This is comparable to the loading of CO_2 in solvent based carbon capture, the amount of CO_2 that can be absorbed within the solvent, typically mol CO_2/mol solvent. A loading value of 1.78% is low in comparison to the typical MEA based loading 0.077-0.354 mol CO_2/mol amine [20], converted to 0.06-0.25 kg CO_2/kg amine. This is due to the high density of the steel bed material in comparison to the gas phase. Altering the concentration of CO_2 in the gas phase would affect the loading respectively by increasing the mass of frost desublimed on the bed material. The loading of CO_2 on bed material is primarily affected by the concentration of CO_2 in the gas phase and the initial

bed temperature of the bed material. Higher CO_2 concentrations and colder bed material temperatures would improve the loading.

Only temperature profiles of the thermocouples that are within the frosted region of the bed will display a plateau indicative of CO_2 frost formation. Ideally the temperature profiles of thermocouples outside the frosted region would remain constant below the frosting temperature as the bed material would have a uniform temperature throughout the entire capture column. This is not the case realistically, however there is a temperature gradient present in the bed material after the cooling step has been completed. The bed material therefore is expected to slowly increase in temperature as frosted bed material is removed from the column and relatively warmer bed material travels down the column.

Figure 6 shows the temperature profiles of thermocouples close to the gas injector as well as a temperature profile calculated from the CO_2 concentration at the frost front. The gas sensor at the outlet of the capture column records the concentration of CO_2 present in the gas leaving the capture column, which is then used to estimate the temperature of the frost front using the Span and Wagner equation of state [21] shown in equation (3). The saturation pressure in equation (3) is compared to the partial pressure of CO_2 in the mixed gas stream, when the saturation pressure is less than the partial pressure of CO_2, CO_2 will desublime out of the gas phase onto the bed material. If the simulated temperature profile closely matches the temperature profile of one of the thermocouples, then the frost front can be assumed to be located close to the region of the bed where that thermocouple is located.

$$ln\left(\frac{P_{sat}}{P_t}\right) = \frac{T_t}{T}\left(a_1\left(1-\frac{T}{T_t}\right) + a_2\left(1-\frac{T}{T_t}\right)^{1.9} + a_3\left(1-\frac{T}{T_t}\right)^{2.9}\right) \quad (3)$$

Where a_1=-14.740846, a_2=2.4327015, a_3=-5.3061778, P_{sat} is the saturation pressure, P_t is the triple point pressure (0.51795 MPa), T_t is the triple point temperature (216.592 K) and T is temperature (K).

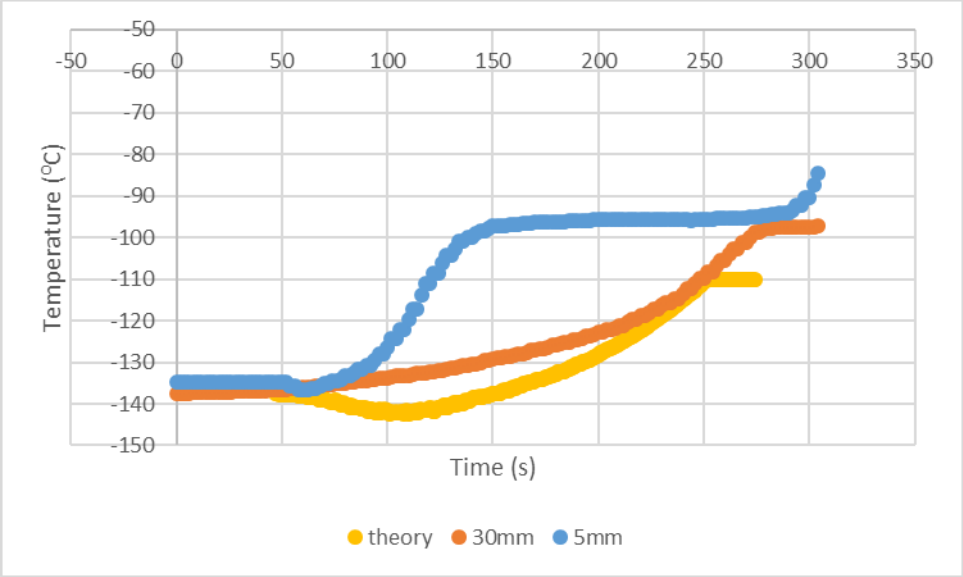

305

306 **Figure 6.** Temperature profiles of thermocouples under moving bed conditions -140°C 18% CO_2

307 0.024 kg/s bed flow (colour)

308

309 The calculated temperature profiles align well with the 30mm thermocouple temperature profile. The

310 5mm temperature profile demonstrates a plateau in figure 6 at roughly -95°C, where the expected

311 desublimation temperature for 18% v/v CO_2 is -97.2°C, which signifies the frost front is present at that

312 point. The 30mm temperature profile does not appear to demonstrate a clear plateau forming. The

313 temperature profiles for 5mm and 30mm under fixed bed conditions (figure 3ai and 3bi) follow a very

314 similar trend, with a plateau forming at the same temperature, whereas this pattern has been

315 interrupted in moving bed experiments. It can be seen that the temperature profile for the 30mm

316 point plateaus at a delayed time in comparison to figure 3. The 30mm plateau in fixed bed experiments

317 forms approximately 70-80s after the 5mm temperature profile plateaus, in the moving bed

318 experiments the 30mm temperature profile plateaus approximate 125s after the 5mm temperature

319 profile. It is most likely that the moving bed is causing this phenomenon by slowing down the frost

320 front velocity in the capture column.

321

It appears that the frost front remains between the 5mm and the 30mm thermocouple, as opposed to advancing through the bed, which would be indicated by the general trend of the simulated temperature profile and the 30mm temperature profile. This would lead to the conclusion that the frost front velocity is being controlled by the movement of the bed. The moving bed experiment has therefore demonstrated that the build-up of CO_2 frost within the capture column can be prevented by continuously removing frosted bed material. The experimental work done in this paper justifies the A3C process being at TRL 3.

Future work will integrate a second injector into the capture column for bed cooling to allow the precooling step and the capture step of the moving bed to occur simultaneously. This is a necessary step in order to progress the development of the cryogenic moving bed, which would require a continuous cycle of the three stages of cryogenic carbon capture: the cooling stage, capture stage and recovery stage. There is also opportunity for the capture column to be tested using different bed materials, such as ceramic and glass beads, comparing the frost front velocities for different bed materials within the capture column. Both areas of future work seek to develop the A3C process to more robust, full system of carbon capture to advance the TRL even further.

4. Conclusion

This work presents the first attempt for CO_2 desublimation using a moving packed bed. Firstly, experiments were conducted in a fixed bed packed bed that helped to derive a simple but effective method to estimate the frost front velocity for CO_2 capture. Secondly the results were used to design a moving bed with a matching bed velocity to allow for effective and continuous separation of CO_2 from gas mixtures. The frost front velocity was found to vary between 0.46-0.78 mm/s with varying CO_2 concentrations ranging from 4%-18% and between 0.37-0.99 mm/s with varying gas superficial velocities ranging from 0.12-0.28 m/s. These experimental results compare well with results from

Tuinier et al. for varying gas flow rates by using correction factors. The comparison for varying concentration showed discrepancies and the need for improvement of the method used.

The moving bed experiments successfully showed that the frost front velocity can be controlled and that the accumulation of frost within the capture column can be prevented under appropriate conditions. The frost covering on the bed material is thin, resulting in a low ratio of CO_2 frost mass to bed material mass, this CO_2 frost loading is dependent on the CO_2 concentration in the gas and can also be improved by reducing the initial bed temperature in the capture column. These findings will lead into further steps to develop the moving bed capture system, with the primary focus being the simultaneous operation of the cooling stage and capture stage within the capture column.

CRediT authorship contribution statement

David Cann: Validation, Formal analysis, Investigation, Writing. **Carolina Font-Palma:** Resources, Writing – review and editing, Visualization, Supervision, Project administration, Funding acquisition. **Paul Willson:** Conceptualization, Resources, Writing – review and editing, Visualization, Supervision, Funding acquisition.

Declaration of competing interest

There are no competing interests in this work.

Acknowledgements

This project is sponsored by PMW Research in conjunction with The University of Chester. The University of Chester is a proud delivery partner of the Eco-Innovation Cheshire and Warrington project which is part-funded by the European Regional Development Fund.

Funding: This work was supported by the European Regional Development Fund [03R16PO1048]; and PMW Research.

References

1. IEAGHG, *Assessment of emerging CO_2 capture technologies and their potential to reduce costs.* 2014/TR4, December 2014.
2. Global CCS Institute, *Global status of CCS 2019*. 2019.
3. Sreenivasulu, B., et al., *A journey into the process and engineering aspects of carbon capture technologies.* Renewable & Sustainable Energy Reviews, 2015. **41**: p. 1324-1350.
4. Benhelal, E., et al., *Global strategies and potentials to curb CO2 emissions in cement industry.* Journal of Cleaner Production, 2013. **51**: p. 142-161.
5. Spitoni, M., et al., *Theoretical evaluation and optimization of a cryogenic technology for carbon dioxide separation and methane liquefaction from biogas.* Journal of Natural Gas Science and Engineering, 2019. **62**: p. 132-143.
6. HM Government., *The Climate Change Act 2008 (2050 amendment) order 2019*. 2019.
7. European Parliament, *Climate Change: European Parliament resolution of 14 March 2019 on climate change – a European strategic long-term vision for a prosperous, modern, competitive and climate neutral economy in accordance with the Paris Agreement (2019/2582(RSP))*. 2019.
8. Haszeldine, R.S., *Carbon Capture and Storage: How Green Can Black Be?* Science, 2009. **325**(5948): p. 1647-1652.
9. Tuinier, M.J., et al., *Cryogenic CO2 capture using dynamically operated packed beds.* Chemical Engineering Science, 2010. **65**(1): p. 114-119.
10. Baxter, L., A. Baxter, and S. Burt, *Cryogenic CO2 Capture as a Cost-Effective CO2 Capture Process.* 2009.
11. Willson, P., et al., *Evaluation of the performance and economic viability of a novel low temperature carbon capture process.* International Journal of Greenhouse Gas Control, 2019. **86**: p. 1-9.
12. Ali, A., et al., *Energy Minimization in Cryogenic Packed Beds during Purification of Natural Gas with High CO2 Content.* Chemical Engineering & Technology, 2014. **37**(10): p. 1675-1685.
13. Song, C.F., Y. Kitamura, and S.H. Li, *Evaluation of Stirling cooler system for cryogenic CO2 capture.* Applied Energy, 2012. **98**: p. 491-501.
14. Song, C.F., et al., *Analysis of CO2 frost formation properties in cryogenic capture process.* International Journal of Greenhouse Gas Control, 2013. **13**: p. 26-33.
15. Tuinier, M.J., M.V. Annaland, and J.A.M. Kuipers, *A novel process for cryogenic CO2 capture using dynamically operated packed beds-An experimental and numerical study.* International Journal of Greenhouse Gas Control, 2011. **5**(4): p. 694-701.
16. Wang, W., et al., *Theoretical study on the critical heat and mass transfer characteristics of a frosting tube.* Applied Thermal Engineering, 2013. **54**(1): p. 153-160.
17. Crawshaw, J.P., W.R. Paterson, and D.M. Scott, *Gas channelling and heat transfer in moving beds of spherical particles.* Chemical Engineering Research & Design, 2000. **78**(A3): p. 465-472.
18. Yoon, S.M. and D. Kunii, *GAS FLOW AND PRESSURE DROP THROUGH MOVING BEDS.* Industrial & Engineering Chemistry Process Design and Development, 1970. **9**(4): p. 559-&.
19. Happel, J., *Pressure Drop Due to Vapor Flow through Moving Beds.* Industrial & Engineering Chemistry, 1949. **41**(6): p. 1161-1174.
20. Afkhamipour, M. and M. Mofarahi, *Review on the mass transfer performance of CO2 absorption by amine-based solvents in low- and high-pressure absorption packed columns.* RSC Advances, 2017. **7**(29): p. 17857-17872.
21. Span, R. and W. Wagner, *A new equation of state for carbon dioxide covering the fluid region from the triple-point temperature to 1100 K at pressures up to 800 MPa.* Journal of Physical and Chemical Reference Data, 1996. **25**(6): p. 1509-1596.